

1 **Revision 3**

2 **Charleshatchettite, $\text{CaNb}_4\text{O}_{10}(\text{OH})_2 \cdot 8\text{H}_2\text{O}$, a new mineral from Mont Saint-Hilaire,**
3 **Québec, Canada: Description, Crystal-Structure Determination and Origin**

4 Monika M.M. Haring and Andrew M. McDonald

5 Department of Earth Sciences, Laurentian University, Sudbury, Ontario P3E 2C6, Canada

6 **Abstract**

7 Charleshatchettite, $\text{CaNb}_4\text{O}_{10}(\text{OH})_2 \cdot 8\text{H}_2\text{O}$, is a new mineral related to franconite and
8 hochelagaite, discovered on a fracture surface of a nepheline syenite at Mont Saint-Hilaire,
9 Québec, Canada. The mineral occurs in white globules (~ 0.15 to 0.20 mm in diameter)
10 composed of radiating crystals with individual crystals having average dimensions of $\sim 0.002 \times$
11 0.010×0.040 mm. Crystals are euhedral, bladed (flattened on [100]) and are transparent to
12 translucent. The mineral is associated with albite, quartz, muscovite, pyrrhotite, pyrite, ancylite-
13 (Ce), and siderite. Charleshatchettite is inferred to be biaxial (-) with $\alpha' = \sim 1.72(2)$ and $\gamma' =$
14 $\sim 1.82(2)$. Data from chemical analyses (SEM-EDS, $n = 8$): CaO 7.96 (7.04 – 8.63), MgO 0.24
15 (0.08 – 0.78), Al_2O_3 0.13 (*b.d.* – 0.49), SiO_2 1.04 (0.49 – 1.88), TiO_2 3.64 (2.45-5.05), Nb_2O_5
16 68.07 (64.83 – 71.01), and H_2O (calc.) 22.96, total 104.04 wt. % gives the average empirical
17 formula: $(\text{Ca}_{1.00}\text{Mg}_{0.04})_{\Sigma=1.04}(\text{Nb}_{3.62}\text{Ti}_{0.32}\text{Si}_{0.12}\text{Al}_{0.02})_{\Sigma=4.08}\text{O}_{10}(\text{OH})_2 \cdot 8\text{H}_2\text{O}$ (based on 20 anions).
18 This is similar to that of hochelagaite ($\text{CaNb}_4\text{O}_{11} \cdot n\text{H}_2\text{O}$), although the two are readily
19 distinguished by their powder X-ray diffraction patterns. Results from single-crystal X-ray
20 diffraction analysis give $a = 21.151(4)$ $b = 6.496(2)$ $c = 12.714(3)$ Å and $\beta = 103.958(3)^\circ$, space
21 group $C2/c$ (#15). The crystal structure, refined to $R = 5.64\%$, contains one *Ca* site, two
22 distorted octahedral *Nb* sites, and ten *O* sites. It consists of clusters of four edge-sharing
23 $\text{Nb}(\text{O},\text{OH})_6$ octahedra, linked through shared corners to adjacent clusters, forming layers of
24 $\text{Nb}(\text{O},\text{OH})_6$ octahedra. These alternate along [100] with layers composed of $\text{Ca}(\text{H}_2\text{O})_8$

25 polyhedra, the two being linked together by H-bonding. Charleshatchettite is a late-stage
26 mineral, interpreted to have developed through the interaction of low T (< 150 °C) aqueous
27 fluids with an alkali-, Nb-rich precursor under slightly reducing conditions and a highly alkaline
28 pH. The precursor mineral(s) is unknown but is considered to have been Nb-dominant, relatively
29 unstable under slightly reducing as well as alkaline conditions, and likely itself would have been
30 a product of near-complete Nb/Ta fractionation due to the paucity of Ta in charleshatchettite.
31 Charleshatchettite is crystallochemically related to SOMS [Sandia Octahedral Molecular Sieves;
32 $\text{Na}_2\text{Nb}_{2-x}\text{M}_x\text{O}_{6-x}(\text{OH})_x \cdot \text{H}_2\text{O}$ with $M = \text{Ti, Zr, Hf}$], a group of synthetic compounds with strong ion
33 exchange capabilities.

34 Keywords: new mineral, charleshatchettite, Mont Saint-Hilaire, SOMS, hochelagaite, franconite,
35 Nb/Ta fractionation, crystal structure

36 Introduction

37 Franconite-group minerals (FGM) are alkali-niobate hydrates that develop as late-stage,
38 low- T minerals in agpaitic environments including Mont-Saint Hilaire (Horváth & Gault 1990),
39 the Saint-Amable sill (Horváth *et al.* 1998), the Khibiny massif (Pekov & Podlesnyi 2004), the
40 Vuoriyarvi alkaline-ultrabasic massif (Belovitskaya & Pekov 2004) and the Vishnevogorsk alkali
41 complex (Nikandrov, 1990). Current members of the FGM include franconite
42 $[\text{Na}(\text{Nb}_2\text{O}_5)(\text{OH}) \cdot 3\text{H}_2\text{O}]$, hochelagaite $(\text{CaNb}_4\text{O}_{11} \cdot n\text{H}_2\text{O}; \text{Jambor } et al. 1986)$, and ternovite
43 $[\text{MgNb}_4\text{O}_{11} \cdot n\text{H}_2\text{O}; \text{Subbotin } et al. 1997]$. The crystal structures and chemical formulas of these
44 minerals are in general, difficult to resolve, primarily owing to their occurrence in thin (< 5 μm)
45 blades, but also because these typically develop into more complex, radiating spheres wherein
46 more than one species may be present. Despite obvious challenges, progress has been made in
47 unravelling the crystal-chemical structures of the FGM, mainly due to advances having been

48 made in single-crystal X-ray diffraction methods. For example, the crystal structure of
49 franconite was solved by Haring & McDonald (2014) who showed the mineral is strongly
50 layered with sheets of $\text{Nb}(\text{O},\text{OH})_6$ polyhedra alternating with sheets $\text{Na}(\text{O},\text{H}_2\text{O})_5$ polyhedra,
51 these being joined by weak H-bonds along [100], and provided a refined chemical formula
52 $\text{Na}(\text{Nb}_2\text{O}_5)(\text{OH})\cdot 3\text{H}_2\text{O}$. The crystal structures of hochelagaite and ternovite still remain unsolved
53 but a combination of data from PXRD and Raman/FTIR spectroscopy suggest they are all
54 closely related.

55 As part of a broader study aimed at better understanding the development of late-stage
56 niobate minerals from agpaitic environments, an investigation of a previously undescribed
57 species believed to be related to minerals of the FGM, was undertaken. This mineral, which
58 serves as the subject of this report, was likely first observed in specimens ($n = 5$) collected by
59 Elsy and Les Horvath in 1978. It was not recognized as a potentially new species until 1985,
60 based on material ($n = 2$) collected in the Poudrette Quarry at Mont Saint-Hilaire, QC by the late
61 Mr. Ron Wadell. The material was found to be a Ca-niobate hydrate, chemically similar to
62 hochelagaite, but with a PXRD pattern distinct from that of the former; it was thus considered as
63 potentially being a new mineral species and given the temporary designation UK56. The very
64 thin nature of its crystals (~ 0.002 mm on average) and evidence for stacking disorder (*e.g.*, X-ray
65 precession images) precluded a complete analysis by single-crystal methods available and so it
66 remained an unidentified mineral for a considerable period of time. However, the advent of
67 extremely bright X-ray sources arising from a combination of rotating-anode generators coupled
68 with multi-layer optics, incident-beam paths, and highly sensitive detectors, has proved
69 invaluable in solving the crystal structures of minerals whose crystal structures would have
70 formerly been challenging if not impossible to solve (Cooper & Hawthorne 2012). An example

71 of just how critical this technology has become is shown in this study of UK56, which is now
72 recognized as the new species, charleshatchettite, $\text{CaNb}_4\text{O}_{10}(\text{OH})_2 \cdot 8\text{H}_2\text{O}$.

73 In this contribution we present and discuss data pertaining to the crystal chemistry of
74 charleshatchettite, elucidate the relationship of the mineral to other members of the FMG,
75 describe the geological conditions under which it is thought to have developed and compare it to
76 synthetic niobate compounds such as Sandia Octahedral Molecular Sieves (SOMS). The mineral
77 is named in recognition of Charles Hatchett (b.1765 – d.1847), an English chemist who
78 discovered niobium, a dominant element in charleshatchettite. Both the mineral and mineral
79 name have been approved by the Commission on New Minerals, Nomenclature and
80 Classification of the International Mineralogical (2015 – 048). The holotype material is housed
81 in the collections of the Canadian Museum of Nature, Gatineau, Québec, under catalogue
82 number CMNMC 86894.

83 Occurrence

84 Charleshatchettite was discovered on a fracture surface on a fine-grained nepheline
85 syenite at the Poudrette quarry, La Vallée-du-Richelieu, Montérégie (formerly Rouville County),
86 Québec, Canada (45°33'8"N, 73°9'3"W). Associated minerals include (in order of decreasing
87 modal abundance) albite, quartz, muscovite, pyrrhotite, pyrite, ancylite-(Ce), and siderite. The
88 mineral has only been found on two samples to date. Owing to the similarity in appearance and
89 physical properties of charleshatchettite to other FGM, the mineral may be present other
90 specimens labelled as hochelagaite or franconite. The fracture surface upon which
91 charleshatchettite occurs is dominated by translucent, white, subhedral, blocky crystals of albite
92 (average dimensions: 0.7 x 1.5 x 2 mm). These are intergrown with transparent crystals of
93 euhedral quartz displaying the forms prism {120} and dipyramid {112} (average dimensions: 0.9
94 x 0.8 x 1.5 mm). Both the quartz and the albite are overgrown by euhedral, colourless, platy

95 crystals of muscovite, which can also be found intergrown with anhedral crystals of pyrrhotite.
96 The pyrrhotite is strongly magnetic, suggesting that it is likely the monoclinic 4C polytype,
97 possibly suggesting a T of formation < 230° C (Kontny et al. 2000). The pyrrhotite is overgrown
98 by euhedral crystals of pyrite displaying the cube {100} and octahedron {111}. Siderite
99 overgrows both the pyrrhotite and the pyrite and can show rusty staining. It develops as euhedral
100 rhombohedra {111} that are tan to light brown (average dimensions 1.0 x 0.8 x 1.2 mm). Rare,
101 euhedral, light pink crystals ancylite-(Ce) (average dimensions: 0.4 x 0.5 x 0.8 mm) overgrow
102 muscovite and pyrrhotite. The associated ancylite-(Ce) is characterized by a bluish-grey
103 fluorescence when exposed to long-, medium, and short-wave radiation. Charleshatchettite is
104 paragenetically the last mineral to develop and can be found overgrowing all the other associated
105 minerals. The general paragenetic sequence involving charleshatchettite is given in Fig. 1.

106 **Physical Properties**

107 Charleshatchettite occurs in white globules ~ 0.15 to 0.20 mm in diameter, composed of
108 radiating crystals (Fig. 2). Individual crystals have average dimensions of ~ 0.07 x 0.02 x 0.01
109 mm and are euhedral, bladed with a perfect [100] cleavage. They are white, transparent to
110 translucent, with a silky lustre, and are flattened on [100] and elongated along [001].
111 Charleshatchettite, like hochelagaite, does not exhibit fluorescence under long-, medium-, or
112 short-wave radiation; this is in contrast with franconite that typically exhibits a distinctive bright
113 yellow-white fluorescence under short-wave and a dull yellow-white fluorescence under long-
114 wave radiation (Horvath & Gault 1990). The Moh's hardness could not be determined due to the
115 small sizes of the crystals. Hochelagaite was estimated to have a Moh's hardness of ~ 4 and
116 given the crystal-chemical similarities between hochelagaite and charleshatchettite,
117 charleshatchettite, likely has a similar hardness. A density of 2.878 g/cm³ was calculated using

118 the empirical chemical formula and unit-cell parameters derived from the crystal-structure
119 analysis.

120 A complete set of optical data as well as an interference figure could not be measured due
121 to the thinness ($\sim 1 \mu\text{m}$) of the crystals the b -axis. The mineral is assumed to be biaxial due to the
122 fact it is monoclinic. It has $\alpha' = \sim 1.72(2)$ perpendicular to the plane of the blades and $\gamma' =$
123 $\sim 1.82(2)$ along the length of the crystals. These values are similar to those of other FGM
124 including hochelagaite [$n_{\text{min}} = 1.72(2)$ and $n_{\text{max}} = 1.82(2)$, Jambor et al. 1986], franconite [$n_{\text{min}} =$
125 $1.72(2)$ and $n_{\text{max}} = 1.79(2)$, Jambor et al. 1984], and ternovite [$n_{\text{min}} = 1.72(2)$ and $n_{\text{max}} = 1.85(2)$,
126 Subbotin 1997]. The mineral is assumed to be optically negative as it has unit cell parameters
127 and refractive indices similar to other FGM which are optically negative. Charleshatchettite is
128 colourless under plane-polarized light with no observed pleochroism. The compatibility index,
129 calculated using the empirical formula and unit-cell parameters derived from the crystal-structure
130 analysis, is 0.055 which is considered good (Mandarino 1981). A combination of the instability
131 of the mineral under the electron beam (leading to elemental loss) and that only two refractive
132 indices could be measured likely influence the less-than-ideal compatibility index.

133 Chemistry

134 Chemical analyses of charleshatchettite were made by energy-dispersive spectrometry
135 with a JEOL JSM 6400 scanning electron microscope operated at a voltage of 20 kV, a beam
136 current of $\sim 1 \text{ nA}$, and a beam width of $1 \mu\text{m}$. The following standards (X-ray lines) were
137 employed: CaTiO_3 ($\text{CaK}\alpha$, $\text{TiK}\alpha$), diopside ($\text{MgK}\alpha$, $\text{SiK}\alpha$), albite ($\text{AlK}\alpha$), and synthetic
138 MnNb_2O_6 ($\text{NbK}\alpha$). Four charleshatchettite-bearing globules were examined in this study and all
139 were found to be a single-phase, *i.e.*, free of other potential Na-dominant phases, including
140 franconite. From the globules, five crystals of charleshatchettite were selected for analysis.
141 Chemical analyses ($n = 8$) of these gave the average (range) compositions: CaO 7.96 (7.04 –

142 8.63), MgO 0.24 (0.08 – 0.78), Al₂O₃ 0.13 (*b.d.* – 0.49), SiO₂ 1.04 (0.49 – 1.88), TiO₂ 3.64
143 (2.45-5.05), Nb₂O₅ 68.07 (64.83 – 71.01), and H₂O (calc.) 22.96, total 104.04 wt. %
144 corresponding to the empirical formula:
145 (Ca_{1.00}Mg_{0.04})_{Σ=1.04}(Nb_{3.62}Ti_{0.32}Si_{0.12}Al_{0.02})_{Σ=4.08}O₁₀(OH)₂•8H₂O (based on 20 anions) or ideally
146 CaNb₄O₁₀(OH)₂•8H₂O. There was insufficient material for direct analysis of H₂O, so the
147 calculated H₂O is based on results from the crystal structure. The mineral was found to be
148 highly unstable under the electron beam, so the high analytical total may be attributed to water-
149 loss during analysis. Additional elements, including Na, Ta and F, were also sought, but not
150 detected. The strongest EDS peak associated with Ta is located at *Lα* 8.145 KeV was absent in
151 the EDS spectrum of charleshatchettite confirming the absence of Ta. Although there is some
152 overlap between peaks in the EDS spectra of Si and Ta, there is a large difference in energy
153 between the strongest peaks of each element (strongest peaks: Ta = *Lα* 8.145 KeV, Si = *Kα* 1.739
154 KeV). The notable absence of Ta, despite the crystal-chemical similarity of Ta and Nb, is
155 consistent with analyses made of other Nb-dominant mineral from agpaitic environments,
156 including those of the FGM (Haring & McDonald 2014).

157 **Raman and Infrared Spectroscopy**

158 The Raman spectrum of charleshatchettite was collected with a Horiba Jobin Yvon
159 XPLORA Raman spectrometer interfaced with an Olympus BX41 microscope using a crystal
160 mounted on a spindle stage and oriented such that the laser was perpendicular to {100}. The
161 spectrum (Fig. 3a) represents an average of three 20 s acquisition cycles, each collected over a
162 range of 50 to 4000 cm⁻¹. The mineral was first analysed using an excitation radiation of $\lambda =$
163 532 nm but this was found to produce fluorescence peaks in the region of ~2500 cm⁻¹, a region
164 that does not typically contain bands attributable to any chemical groups in most minerals. To

165 evaluate this further, the mineral was instead analysed using an excitation radiation of $\lambda = 638$
166 nm; this eliminated all peaks in the region, suggesting they were indeed products of fluorescence.
167 A grating of 1200 lines/cm and a 40x long working distance objective were also used, producing
168 a beam of diameter $\sim 2 \mu\text{m}$. Calibration was made using the 521 cm^{-1} line of a silicon wafer.
169 The Raman spectrum of charleshatchettite shows bands in the regions of 2900 – 3600, 1400 –
170 1500, 1000 - 850, 670 - 475 and 470 - 50 cm^{-1} (Table 1) (Fig. 2a). The first region at 2900 –
171 3600 cm^{-1} contains three moderately sharp to broad, weak to moderate intensity peaks at 3314,
172 3046, and 2939 cm^{-1} that are attributed to O-H bending (Williams 1995). In the region of 1400 –
173 1500 cm^{-1} , a weak low-intensity peak occurs at 1459 cm^{-1} , ascribed to H-O-H bending. The
174 region of 1000 to 850 cm^{-1} contains two strong, sharp peaks at 930 - 878 cm^{-1} that can be
175 attributed to the symmetric stretching of Nb=O double bonds (Jehng & Wachs 1990; Haring &
176 McDonald 2014). The region between 670 - 475 cm^{-1} contains two strong sharp bands at 658
177 and 599 cm^{-1} that are attributed to symmetric stretching of Nb-O-Nb bonds (Jehng & Wachs
178 1990; Haring & McDonald 2014). Finally, the region at 470 - 50 cm^{-1} contains seven low to
179 moderate intensity peaks at 489, 378, 234, 215, 205, 150, and 115 cm^{-1} attributed to Ca-O bonds
180 (Williams 1995). To confirm these band assignments, a Raman spectrum was calculated using
181 results from the refined crystal structure (described below) along with the programs GAUSSIAN
182 (Frisch *et al.* 2013) to calculate force constants for each bond, and VIBRATZ (Dowty 2009) to
183 determine and refine the calculated Raman spectrum (Table 1). Results show an overall good
184 agreement between the experimental and calculated Raman spectra in terms of both band
185 position and intensity (Table 1). As a note, those peaks associated with O-H and H-O-H bending
186 could not be determined for the calculated Raman spectrum owing to the fact that the site(s)
187 occupied by H could not be reliably determined from the refined crystal structure. The Raman

188 spectra for charleshatchettite and hochelagaite are compared in Figure 3b. These show that the
189 spectra of the two minerals are virtually indistinguishable from one another; this is predictable,
190 owing to strong chemical and crystal-structure similarities between the two. However, it does
191 indicate that Raman spectroscopy cannot be used to reliably distinguish between them.

192 The presence of water in charleshatchettite was further investigated by infrared
193 spectroscopy, given that water is a weak Raman scatterer but a strong absorber of infrared
194 radiation. An infrared (FTIR) spectrum (Fig. 4) over the range of 600 to 4000 cm^{-1} was
195 collected using a Bruker Alpha spectrometer equipped with a KBr beam splitter and a DTGS
196 detector. This spectrum, obtained by averaging 128 scans with a resolution of 4 cm^{-1} , reveals
197 three distinct bands in the regions of $\sim 3700 - 2800$, $1700 - 1300$, and $1200 - 650 \text{ cm}^{-1}$ (Table
198 2). The region at $\sim 3700 - 2800 \text{ cm}^{-1}$ consists of broad, high intensity peak at 3362 cm^{-1} as well
199 as two sharp, moderate intensity peaks at 2923 and 2852 cm^{-1} associated with O-H bending
200 (Williams 1995). The second region at $\sim 1700 - 1300 \text{ cm}^{-1}$ consists of a sharp peak at 1654 and
201 1450 cm^{-1} as well as a sharp lower intensity peak at 1384 cm^{-1} associated with H-O-H
202 bending and atmospheric CO_2 , respectively. The third region at $1200 - 650 \text{ cm}^{-1}$ consists of two
203 sharp, high intensity peaks at 934 and 874 cm^{-1} , as well as lower intensity peaks at 1100 , 1025 ,
204 755 , and 697 cm^{-1} . The bands in this region are similar to those in the IR spectra of franconite
205 $[\text{Na}(\text{Nb}_2\text{O}_5)(\text{OH})\cdot 3\text{H}_2\text{O}]$ with peaks at 1025 , 934 and 874 cm^{-1} associated with possible Nb=O
206 double bonds and the peaks at 755 and 697 cm^{-1} associated with Nb-O-Nb single bonds (Fielicke
207 *et al.* 2003, Haring & McDonald 2014). The weak peak at 1100 cm^{-1} , attributed to a Si-O
208 asymmetric stretch, is considered to be due to trace amounts of silicates such as quartz or albite,
209 both of which are associated with charleshatchettite. There is overall good agreement between
210 the complimentary Raman and FTIR spectra collected for charleshatchettite. The low-intensity

211 peak observed at 1459 cm^{-1} in the Raman spectrum of charleshatchettite, attributed to H-O-H
212 bending, corresponds to the peak at 1450 cm^{-1} in the FTIR spectrum. Other bands observed in
213 the Raman spectrum of charleshatchettite that correspond to those present in the FTIR spectrum
214 include those in the regions of $2900 - 3600\text{ cm}^{-1}$ (O-H bending) as well as $1000 - 850$ (Nb=O
215 bonds). However, given the chemical and structural similarities among FGM, the Raman spectra
216 of these minerals are virtually identical, all with two sharp, strong peaks in the regions of $1000 -$
217 850 and $670 - 475\text{ cm}^{-1}$ (Nb-O bonds) as well as a broad peak in the region of $2900 - 3600\text{ cm}^{-1}$.

218 **X-ray Crystallography and Crystal-Structure Determination**

219 X-ray powder diffraction data were collected using a 114.6 mm diameter Gandolfi
220 camera, a 0.3 mm collimator, and Fe-filtered $\text{CoK}\alpha$ radiation ($\lambda = 1.7902\text{ \AA}$). Intensities were
221 determined using a scanned image of the pattern and normalized to the measured intensity of $d =$
222 10.308 \AA ($I = 100$). The measured intensities were compared to a pattern calculated using results
223 from the crystal-structure analysis and the program CRYSCON (Dowty 2002) and overall, there
224 is a good agreement between the two (Table 3). It is worth noting that charleshatchettite and
225 hochelagaite have significantly different PXRD patterns (Table 3), making distinguishing
226 between them straightforward and supporting them as being distinct species.

227 To obtain a crystal suitable for single-crystal XRD, individual crystals were separated
228 from a coarse-grained, charleshatchettite-bearing globule and examined optically with a
229 polarizing-light microscope. From these, a crystal with the dimensions $0.09 \times 0.03 \times 0.01\text{ mm}$,
230 exhibiting a simple extinction and no evidence for twinning was selected. X-ray intensity data
231 were collected on a Bruker D8 three-circle diffractometer equipped with a rotating-anode
232 generator, multi-layer optics incident beam path and an APEX-II CCD detector. X-ray
233 diffraction data were collected to $60^\circ 2\theta$ using 20 s per 0.3° frame and with a crystal-to-detector

234 distance of 5 cm. The unit-cell parameters for charleshatchettite, obtained by least-squares
235 refinement of 4160 reflections ($I > 10\sigma I$), are $a = 21.151(4)$ $b = 6.496(2)$ $c = 12.714(3)$ Å and β
236 $= 103.96(3)^\circ$ (Table 4), are very similar to those of hochelagaite (Table 5). An empirical
237 absorption correction (SADABS; Sheldrick, 1997) was applied and equivalent reflections
238 merged to give 1106 unique reflections covering the entire Ewald sphere.

239 Solution and refinement of the crystal structure of charleshatchettite were done using
240 SHELXL-97 (Sheldrick 1997). The crystal structure was solved using direct methods, using the
241 scattering curves of Cromer & Mann (1968) and the scattering factors of Cromer & Liberman
242 (1970). Phasing of a set of normalised structure factors gave a mean value of $|E^2 - 1|$ value of
243 0.908, consistent with a center of symmetry being present $\{|E^2 - 1| = 0.968$ for centrosymmetric,
244 $|E^2 - 1| = 0.736$ for non-centrosymmetric}. Based on this and the space-group choices available,
245 $C2/c$ (#15) was chosen as the correct space group. Phase-normalised structure factors were used
246 to give a Fourier difference map from which two Nb , and several O sites were located. The Ca
247 site and additional O sites were identified from subsequent Fourier difference maps.
248 Refinement of the site-occupancy factors (SOF) indicated that all of the cation and anion sites
249 were fully occupied (Table 6). Determination of which O sites were occupied by OH or H_2O
250 was based on a bond-valence analysis (Table 7). Some of the O sites were found to have low
251 bond-valence sums (*i.e.*, $BVS = 1.500 - 1.800$ *v.u.*) probably due to the presence of OH at these
252 sites. Hydrogen sites were located for OH as well as the OW7, OW8, and OW10 groups
253 however, the H atom sites could not be located for the OW9 site. This is due to the positional
254 disorder of the oxygen associated with OW9. Refinement of this final model converged to $R =$
255 5.39 % and $wR^2 = 13.89$ %.

256

257

Description of Crystal Structure

258

Cation Polyhedra

259 The crystal structure of charleshatchettite contains one unique *Ca* site and two *Nb* sites.

260 Results from the refined-crystal structure and EMPA data indicate that both the *Ca* and *Nb* sites

261 are fully occupied. The *Ca* site is [8]-coordinated by four crystallographically distinct H₂O

262 groups, forming Ca(H₂O)₈ polyhedron. Of the H₂O groups, one in particular, OW9, showed a

263 pronounced electron density spread of 0.64 Å along [010]; it was subsequently modelled as a

264 split site, OW9a and OW9b (Table 6). Refinement of this model gave SOFs of 0.63(2) and

265 0.37(3) for the two split sites, suggesting a relatively high degree of disorder for the OW9 site.

266 There are two *Nb* sites both in octahedral coordination with O atoms and OH groups:

267 Nb(1)O₅(OH) and Nb(2)O₄(OH)₂. The two Nb polyhedra are highly distorted with Nb-(O,OH)

268 bond lengths ranging from 1.749(2) to 2.352(9) Å and 1.823(9) to 2.281(9) Å, respectively

269 (Table 8); this range is consistent with the range in Nb-O bond distances previously observed in

270 franconite (Haring & McDonald 2014) and in other Nb-bearing minerals. These distorted

271 octahedra are likely the result of edge sharing Nb octahedra (see discussion below) which

272 contain a highly charged cation. In both Nb polyhedra, the longest bonds are associated with

273 Nb-OH bonds whereas the shortest bonds are associated with Nb-O bonds.

274

Bond Topology

275 The Nb polyhedra are linked through shared edges to form four-membered clusters

276 composed of two Nb(1)O₅(OH) and two Nb(2)O₄(OH)₂ octahedra (Fig. 5). Each cluster is

277 subsequently linked to six adjacent clusters through shared corners generating 4 x 4 Å pore

278 spaces and forming infinite sheets parallel to [100]. The sheets parallel to [100] correlate with

279 the flattened aspect of crystals and the perfect cleavage in that direction. The layers of

280 Nb(O,OH)₆ octahedra alternate with those containing Ca(H₂O)₈ polyhedra along [100] with an
281 interlayer spacing of ~ 4 Å (Fig. 6).

282 Related Structures

283 The crystal structure of charleshatchettite is topologically similar to that of franconite
284 (Haring & McDonald 2014). Both minerals are hydrous with an [Nb₂O₅(OH)]⁻¹ group, the two
285 differing by the type of interlayer cation between the [Nb₂O₅(OH)]⁻¹ sheets: charleshatchettite
286 having Ca(H₂O)₈ polyhedra and franconite with NaO(H₂O)₄ polyhedra (Haring & McDonald
287 2014). The presence of Ca(H₂O)₈ polyhedra in charleshatchettite and the flipping in the
288 octahedral layers correlates with a doubling of the *a* dimension to 21.151 Å compared to
289 franconite where *a* = 10.119 Å as there are additional H₂O groups coordinated with Ca compared
290 with Na in NaO(H₂O)₄. Both charleshatchettite and franconite possess crystal structures with
291 layers of A(H₂O)₅₋₈ (A = Na,Ca) linked to layers of Nb(O,OH)₆ octahedra through H-bonds along
292 [100], the latter producing the perfect [100] cleavage observed in these minerals. Chemically,
293 charleshatchettite [CaNb₄O₁₀(OH)₂·8H₂O] most closely resembles hochelagaite
294 (CaNb₄O₁₁·*n*H₂O), but as mentioned above, the two have unique PXRD patterns (Table 3). The
295 crystal structure of hochelagaite is unknown but is presumed to be similar to those of franconite
296 and chaleshatchettite. It is however noteworthy that the PXRD pattern for hochelagaite has
297 systematic extinctions that support the mineral having a *P*-lattice, which is different from the *C*-
298 lattice in charleshatchettite. The difference in lattice types between the two may be attributed to
299 the higher proportion of H₂O groups in charleshatchettite relative to hochelagaite.

300 The crystal structure of charleshatchettite is broadly similar to those of the synthetic
301 compounds Na₂Nb₄O₁₁ (Masó *et al.* 2011) and KCa₂Nb₃O₁₀ (Fukoka *et al.* 2000, Jehng & Wachs
302 1990) and Sandia Octahedral Molecular Sieves (SOMS) [Na₂Nb_{2-x}Ti_xO_{6-x}(OH)_x·H₂O (*x* = 0.04 to

303 0.40); Nyman *et al.* 2001]. These compounds have strongly layered structures where layers of
304 $\text{Nb}(\text{O},\text{OH})_x$ ($X = 6$ or 7) polyhedra alternate with layers of MO_x ($X = 6$ or 7 ; $M = \text{Na}, \text{K},$ and Ca)
305 polyhedra. Both SOMS and $\text{Na}_2\text{Nb}_4\text{O}_{11}$, like charleshatchettite, are monoclinic in symmetry and
306 crystallize in the space group $C2/c$ (Nyman *et al.* 2001; Masó *et al.* 2011), whereas $\text{KCa}_2\text{Nb}_3\text{O}_{10}$
307 is orthorhombic, crystallizing in the space group $Cmcm$ (Fukoka *et al.* 2000). Unlike the
308 structures of SOMS and charleshatchettite, $\text{KCa}_2\text{Nb}_3\text{O}_{10}$ is considered to have a layered
309 perovskite-type structure where slabs of corner-sharing NbO_6 octahedra and Ca ions alternate
310 along $[010]$ with layers of K ions (Fukoka *et al.* 2000). In the case of $\text{Na}_2\text{Nb}_4\text{O}_{11}$, layers of edge-
311 sharing $(\text{Nb},\text{Ta})\text{O}_7$ polyhedra alternate with layers composed of edge-sharing NaO_7 and
312 $(\text{Nb},\text{Ta})\text{O}_6$ polyhedra (Masó *et al.* 2011). Of the synthetic compounds, charleshatchettite is most
313 crystallochemically similar to SOMS. The crystal structures of SOMS contain NbO_6 polyhedra
314 consisting of a short bond of $\sim 1.8 \text{ \AA}$, a long bond of $\sim 2.4 \text{ \AA}$ as well as four equatorial bonds with
315 distances of $\sim 2 \text{ \AA}$ (Nyman *et al.* 2002), similar to the $\text{Nb}(1)\text{O}_5(\text{OH})$ polyhedra in
316 charleshatchettite. These NbO_6 octahedra, like those in charleshatchettite, form four-membered
317 clusters through shared edges. Adjacent four-membered NbO_6 clusters do not link to form
318 infinite NbO_6 sheets as in charleshatchettite, but are instead linked to double chains of NaO_6
319 octahedra through shared edges. The four-membered NbO_6 clusters and NaO_6 double chains
320 occur in discreet layers which alternate with one another along $[001]$ (Xu *et al.* 2004). As in
321 charleshatchettite, the crystal structures of SOMS are linked together in part by H-bonds and are
322 able to adsorb extra water into its structure. The amount of H-bonding in the structures of SOMS
323 increase with increasing Ti substitution for Nb due to the substitution reaction $\text{Ti}^{4+} + \text{OH}^- \leftrightarrow$
324 $\text{Nb}^{5+} + \text{O}^{2-}$, whereby more OH groups are added with the addition of Ti into the structure
325 (Nyman *et al.* 2002). The compounds $\text{Na}_2\text{Nb}_4\text{O}_{11}$ and $\text{KCa}_2\text{Nb}_3\text{O}_{10}$ have been synthesized at

326 high temperatures (~1100 – 1300 °C) while SOMS have been hydrothermally synthesized under
327 conditions of at low T (~ 175 °C) and high alkalinity (pH ~ 13.7) (Xu *et al.* 2004). However,
328 increasing the Ti content in SOMS increases the range in T over which the structures are stable: a
329 20% Ti substitution for Nb results in the structures being stabilized up to 576 °C (Nyman *et al.*
330 2002). The compounds $\text{Na}_2\text{Nb}_4\text{O}_{11}$ and $\text{KCa}_2\text{Nb}_3\text{O}_{10}$ have distinct ferroelectric and dielectric
331 properties (Masó *et al.* 2011, Yim *et al.* 2013). On the other hand SOMS, exhibit a strong ion-
332 exchange selectivity for R^{2+} cations over R^+ cations, making them useful in removing heavy
333 metals such as Pb^{2+} , Co^{2+} and Cd^{2+} from ground water and soils (Nyman *et al.* 2001), these being
334 trapped in pores of the Nb clusters. Due to the strong crystallochemical similarities between
335 charleshatchettite and SOMS, charleshatchettite is expected to have similar cation exchange
336 properties. Such cation exchange properties are supported by the range of chemistries observed
337 for FGM [*i.e.*, incorporation of Na, Ca, Mg, +/- Sr, +/- Fe^{2+} into FGM structures; Jambor *et al.*
338 1984, Jambor *et al.* 1986, Subbotin *et al.* 1997, Haring & McDonald 2014].

339

340

Origin and Conditions of Formation

341 Paragenetically, charleshatchettite is a late-stage phase found overgrowing earlier
342 formed phases including, albite, quartz, siderite, muscovite, pyrrhotite and ancylite-(Ce). The
343 mineral, due its hydrous composition, is inferred to have precipitated from aqueous fluids.
344 Previous studies of franconite and hochelagaite, using results from microprobe and mass
345 spectrometry, have shown that the water content can be variable in these minerals, with the
346 number of H_2O groups (*apfu*) ranging from 3 - 26 for franconite and 3 – 9 for hochelagaite
347 (Jambor *et al.* 1984, 1986). Previous heating experiments of Jambor *et al.* (1984) on franconite
348 to temperatures of 150, 250, 350, and 500 °C coupled with PXRD data, reveal a gradual collapse

349 of the structure up to 500 °C at which point the material was found to give a PXRD consistent
350 with that of Na₂Nb₄O₁₁. The collapse of the franconite structure is attributed to the loss of H₂O
351 groups: the removal of H₂O groups would result in the loss of H-bonding that bind layers of
352 Nb(O,OH)₆ octahedra to layers of Na(O,H₂O)₅ polyhedra, thus leading to structural collapse. As
353 H-bonds are essential in stabilizing the crystal structure of franconite, they are also inferred to be
354 equally important in stabilizing the crystal structure of charleshatchettite. It follows, therefore,
355 that heating of charleshatchettite should also lead to a collapse in the crystal structure similar to
356 that observed to in franconite. Given the ease with which franconite loses its structurally bound
357 H₂O and the fact that charleshatchettite shows a greater degree of hydration (H₂O_{calc} = 22.96 wt.
358 %) relative to hochelagaite (H₂O_{calc} = 13.20 wt. %), it is possible that charleshatchettite formed
359 at either a lower *T* (< 150 °C) or under conditions of higher *a*H₂O, relative to hochelagaite. The
360 presence of coexisting siderite and pyrrhotite suggest that the fluids were slightly reducing (Eh =
361 0.0 to -0.4) with a neutral to slightly basic pH (pH = 7 to 8) [at a *T* of 25 °C] (Vaughan 2005;
362 Faure 1991). Due to the crystallochemical similarities between charleshatchettite and SOMS and
363 the fact that SOMS are synthesized at a very high pH, it is probable that the fluids from which
364 charleshatchettite precipitated were also highly alkaline.

365

366

Genetic Implications

367 Charleshatchettite has strong crystallochemical similarities to other FGM and as such
368 should be considered a new member. This broadens the number of related minerals and
369 demonstrates the crystal-chemical flexibility of FGM crystal structure. Although the crystal
370 structures of the FGM are flexible, no Ti- or Zr-dominant members of the FGM have been found
371 to date, despite Ti and Zr having valences and atomic radii (^[6]Ti⁴⁺ = 0.61 Å, ^[6]Zr⁴⁺ = 0.72 Å)

372 similar to those of Nb ($^{[6]}\text{Nb}^{5+} = 0.64 \text{ \AA}$) [Shannon 1976]. The SOMS can incorporate other
373 high-field strength elements like Ti and Zr through the substitution: Ti^{4+} (or Zr^{4+}) + $\text{OH}^- \leftrightarrow \text{Nb}^{5+}$
374 + O^{2-} (Nyman *et al.* 2002, Xu *et al.* 2004). In light of the crystal-chemical similarities between
375 SOMS and charleshatchettite, the occurrence of Ti- or Zr-dominant FMG would seem plausible;
376 however such phases have yet to be discovered. It is noteworthy that the crystal structure of
377 SOMS can only incorporate up to 20% Ti or Zr after which the octahedral sites become
378 increasingly distorted and disordered as observed in the broadening of octahedral peaks in the
379 infrared spectrum of SOMS (Nyman *et al.* 2002). The degree of Ti/Nb substitution in FGM
380 varies from 0.25 to 8.00 %, suggesting that a similar distortion and disordering of the octahedral
381 sites may occur in charleshatchettite; this may thus preclude the crystallization of Ti- and Zr-rich
382 members of the FGM. Incorporation of Ti may also proceed through the substitution $\text{Ti}^{4+} + \text{OH}^-$
383 $\leftrightarrow \text{Nb}^{5+} + \text{O}^{2-}$; such a substitution in charleshatchettite is supported by the fact that some of the O
384 sites are have low bond-valence sums (i.e., $\text{BVS} \sim 1.5 - 1.8 \text{ v.u.}$), suggesting the presence of
385 mixed O/OH sites.

386 Charleshatchettite is a late-stage mineral that probably developed from a Nb-rich
387 precursor that would have been unstable in the presence of highly alkaline, slightly reducing,
388 aqueous fluids. Presumably, the precursor mineral itself would have been both Nb-dominant and
389 virtually devoid of Ta, similar to the chemistry of charleshatchettite. A similar paucity of Ta is
390 observed in other Nb-rich minerals such as vuonnemite $[\text{Na}_{11}\text{Ti}^{4+}\text{Nb}_2(\text{Si}_2\text{O}_7)_2(\text{PO}_4)_2\text{O}_3(\text{F},\text{OH})$;
391 Ercit *et al.* 1998], epistolite $[\text{Na}_4\text{Nb}_2\text{Ti}^{4+}(\text{Si}_2\text{O}_7)_2\text{O}_2(\text{OH})_2(\text{H}_2\text{O})_4$; Sokolova & Hawthorne 2004],
392 laurentianite $\{[\text{NbO}(\text{H}_2\text{O})]_3(\text{Si}_2\text{O}_7)_2[\text{Na}(\text{H}_2\text{O})_2]_3$; Haring *et al.* 2012}, and franconite
393 $[\text{NaNb}_2\text{O}_5(\text{OH})\cdot 3\text{H}_2\text{O}$; Haring & McDonald 2014], laurentianite (from agpaite environments,
394 suggesting that Ta and Nb must undergo significant fractionation prior to late-stage

395 crystallization in agpaitic environments. Possible precursor minerals to charleshatchettite
396 include pyrochlore- or eudialyte-group minerals or possibly vuonnemite. Interactions of fluids
397 with these precursor minerals, especially vuonnemite which is highly susceptible to weathering
398 (Khomyakov *et al.* 1975b, Bussen *et al.* 1978), would have led to an Nb-enrichment of these the
399 fluids. Evidence for the mobility of Nb in agpaitic environments can be seen in the paragenetic
400 relationship between the Nb minerals laurentianite ($[\text{NbO}(\text{H}_2\text{O})]_3(\text{Si}_2\text{O}_7)_2[\text{Na}(\text{H}_2\text{O})_2]_3$) and
401 franconite, whereby laurentianite overgrows the latter (Haring & McDonald 2012). In addition
402 to Nb-enrichment, these fluids could have also been enriched in Ca possibly due to interaction
403 with the carbonate rocks into which the Mont Saint-Hilaire syenites intruded.

404

405

Acknowledgements

406 Our thanks to F.C. Hawthorne (Dept. of Geological Sciences, University of Manitoba) for
407 providing access to the four-circle diffractometer and to Mark. C. Cooper for providing
408 assistance with the single crystal XRD data collection. In addition we thank Dr. Joy Gray-
409 Munro (Department of Chemistry & Biochemistry, Laurentian University) for providing access
410 to the infrared spectrometer as well as assistance with the data collection. We also acknowledge
411 the comments made by Dr. Anthony Kampf and those of the associate editor,
412 Dr. Beda Hofmann. Financial support for this research was provided through a grant to AMM
413 from the Natural Sciences and Engineering Research Council as well as an Alexander Graham
414 Bell Canada Graduate Scholarship to MMMH also from the Natural Sciences and Engineering
415 Research Council.

416

References

417 Brese, N.E. & O'Keeffe, M. (1991) Bond-valence parameters for solids. *Acta Crystallographica*,
418 B47, 192-197.

- 419 Bussen, I.V., Es'kova, E.M., Men'shikov, Yu.P., *et al.* (1978) The mineralogy of hyperalkaline
420 pegmatites. *Problems of Geology of Rare Elements*, M., 251-271.
- 421 Chao, G.Y., Conlon, R.P. and VanVelthuisen, J. (1990) Mont Saint-Hilaire unknowns.
422 *Mineralogical Record*, 21, 363-368.
- 423 Cromer, D.T. & Liberman, D. (1970) Relativistic calculation of anomalous scattering factors for
424 X rays. *Journal of Physical Chemistry*, 53, 1891-1898.
425
- 426 Cromer, D.T. & Mann, J.B. (1968) X-ray scattering factors computed from numerical Hartree-
427 Fock wave functions. *Acta Crystallographica*, A24, 321-324. *ces*, 44: 1333-1346.
428
- 429 Dowty, E. (2009) *VIBRATZ for Windows and Macintosh Version 2.2*. Shape Software
430 Kingsport, Tennessee, USA.
431
- 432 Dowty, E. (2002) *CRYSCON for Windows and Macintosh Version 1.1*. Shape Software
433 Kingsport, Tennessee, USA.
434
- 435 Ercit, T.S., Cooper, M.A. and Hawthorne, F.C. (1998) The crystal structure of vuonnemite,
436 $\text{Na}_{11}\text{Ti}^{4+}\text{Nb}_2(\text{Si}_2\text{O}_7)_2(\text{PO}_4)_2\text{O}_3(\text{F},\text{OH})$, a phosphate-bearing sorosilicate of the
437 lomonosovite group. *Canadian Mineralogist*, 36, 1311-1320.
- 438 Faure, G. (1991) *Principles and applications of geochemistry* 2nd ed. Prentice Hall. pp 243.
439
- 440 Frisch, M. J., Trucks, G. W. Schlegel, H. B., *et al.* (2013) *Gaussian 09, Revision D.01*. Gaussian,
441 Inc., Wallingford CT.
- 442 Haring, M.M. & McDonald A.M. (2014) Franconite, $\text{NaNb}_2\text{O}_5(\text{OH})\cdot 3\text{H}_2\text{O}$: structure
443 determination and the role of H bonding, with comments on the crystal chemistry of
444 franconite-related minerals. *Mineralogical Magazine*, 78, 591-607.
445
- 446 Haring, M.M.M., McDonald, A.M., Cooper, M.A. and Poirier, G.A. (2012) Laurentianite,
447 $[\text{NbO}(\text{H}_2\text{O})]_3(\text{Si}_2\text{O}_7)_2[\text{Na}(\text{H}_2\text{O})_2]_3$, a new mineral from Mont Saint-Hilaire, Québec:
448 description, crystal-structure determination and paragenesis. *The Canadian Mineralogist*,
449 50, 1265-1280.
450
- 451 Horváth, L. and Gault, R.A. (1990) The mineralogy of Mont Saint-Hilaire Québec.
452 *Mineralogical Record*, 21, 284-359.
- 453 Jambor, J.L., Sabina, A.P., Roberts, A.C., Bonardi, M., Owens, D.R. and Sturman, B.D. (1986)
454 Hochelagaite, a new calcium-niobium oxide mineral from Montreal, Québec. *Canadian*
455 *Mineralogist*, 24, 449-453.
- 456 Jehng, J.M. and Wachs I.E. (1990) Structural chemistry and Raman spectra of niobium oxides.
457 *Chemistry of Materials*, 3, 101-107.

- 458 Khomyakov, A.P., Semenov, E.I., Es'kova, E.M., *et al.* (1975b) Vuonnemite from Lovovzero.
459 Iz.AN,ser.geol, 8, 78-87.
- 460 Kontny, A., de Wall, H., Sharp, T.G., and Posfai, M. (2000) Mineralogy and magnetic behavior
461 of pyrrhotite from a 260°C section at the KTB drilling site, Germany. American
462 Mineralogist, 85, 1416 – 1427.
- 463 Mandarino J. A. (1981) The Gladstone–Dale relationship. IV. The compatibility concept and its
464 application. Canadian Mineralogist, 19,441-450.
- 465 Masó, N., Woodward, D.I., Várez, A. and West, A.R. (2011) Polymorphism, structural
466 characterization and electrical properties of Na₂Nb₄O₁₁. Journal of Material Chemistry,
467 21, 12096-12102.
- 468 Nyman, M., Tripathi, A., Parise, J.B., Maxwell, R.S., Harrison, W.T.A. and Nenoff, T.M. (2001)
469 A new family of octahedral molecular sieves: Sodium Ti/Zr^{IV} niobates. Journal of the
470 American Chemical Society, 123, 1529-1530.
- 471 Shannon, R.D. (1976) Revised effective ionic radii and systematic studies in interatomic
472 distances in halides and chalcogenides. Acta Crystallographica, A32, 751-767.
473
- 474 Sokolova, E. and Hawthorne, F.C. (2004) The crystal chemistry of epistolite. Canadian
475 Mineralogist, 42, 797-806.
- 476 Subbotin, V.V., Voloshin, A.V., Pakhomovskii, Y.A., Men'shikov, Y.P. and Subbotina, G.F.
477 (1997) Ternovite, (Mg,Ca)Nb₄O₁₁•nH₂O, a new mineral and other hydrous tetranibates
478 from carbonatites of the Vuoriyarvi massif, Kola Peninsula, Russia. Neues Jahrbuch für
479 Mineralogie, 2, 49-60.
- 480 Vaughan, D. J., (2005) Minerals/Sulphides. In Encyclopedia of geology. Amsterdam: Elsevier,
481 574–586.
482
- 483 Williams, Q. (1995) Infrared, Raman and optical spectroscopy of Earth materials. Pp. 291 -302
484 in: Mineral Physics and Crystallography: a Handbook of Physical Constants (T.J. Ahrens,
485 editor), AGU Reference Shelf Vol 2. American Geophysical Union, Washington, D.C.
486
- 487 Xu, H., Nyman, M., Nenoff, T.M. and Navrotsky, A. (2004) Prototype sandia octahedral
488 molecular sieve (SOMS) Na₂Nb₂O₆•H₂O: Synthesis, structure and thermodynamic
489 stability. Chemistry of Materials, 16, 2034-2040.
- 490 Yim, H., Yoo, S., Nahm, S., Hwang, S., Yoon, S. and Choi, J. (2013): Synthesis and dielectric
491 properties of layered HCa₂Nb₃O₁₀ structure ceramics. Ceramics International, 39, 611-
492 614.
- 493

- 1 Figure 1. Mineral paragenesis for charleshatchettite.
- 2 Figure 2. Globules of charleshatchettite with muscovite, siderite, and pyrrhotite.
- 3 Figure 3a. Raman spectrum for charleshatchettite perpendicular to [100].
- 4 Figure 3b. Raman spectra for charleshatchettite and hochelagaite.
- 5 Figure 4. FTIR spectrum for charleshatchettite.
- 6 Figure 5. The crystal structure of charleshatchettite viewed along [100]. The Nb(1)O₅(OH)
7 (blue) and Nb(2)O₄(OH)₂(pink) octahedra are linked through shared edges to form four-
8 membered clusters. The clusters are then joined through shared corners to adjacent ones, leading
9 to development of infinite sheets in the *b-c* plane.
- 10 Figure 6. The crystal structure of charleshatchettite viewed along [010]. Layers composed of
11 Nb(O,OH)₆ octahedra alternate along [100] with layers composed of Ca atoms (orange) and H₂O
12 (light blue). Weak H-bonding between the layers results in the perfect {100} cleavage observed
13 in the mineral.
- 14
- 15
- 16

Figure 1.

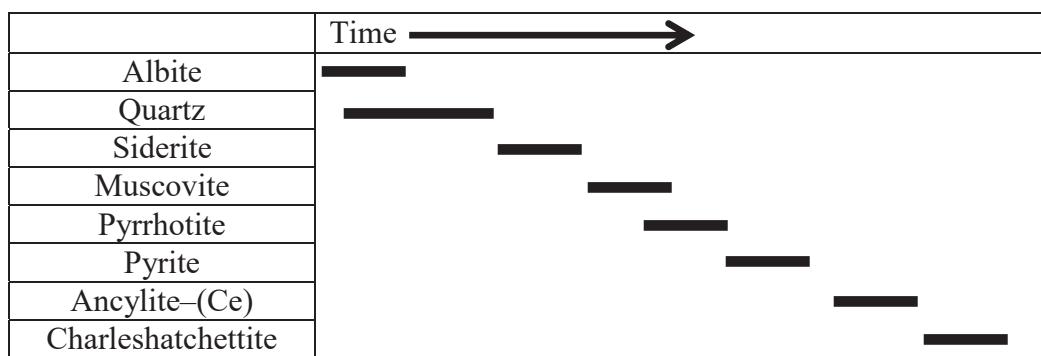


Figure 2

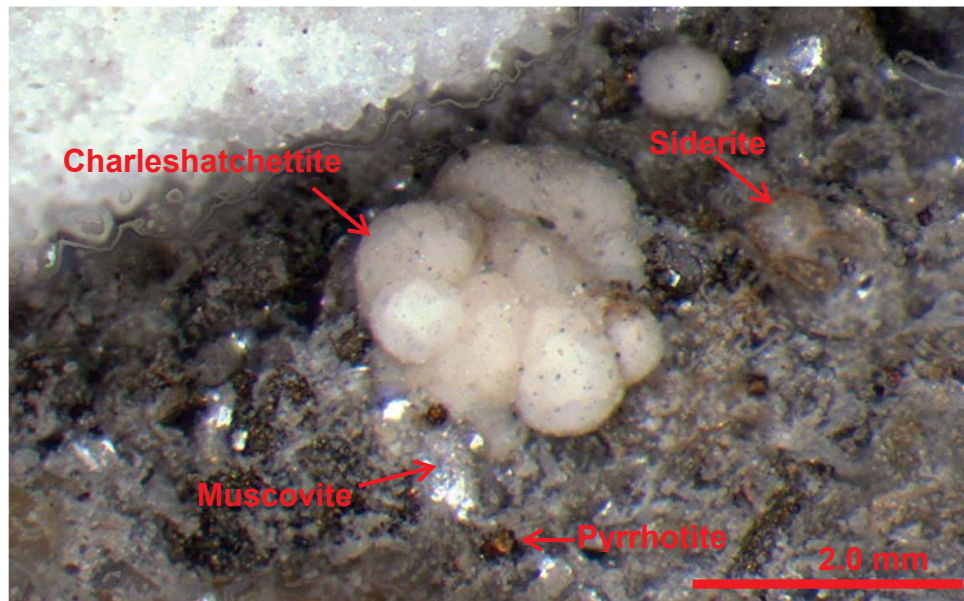


Figure 3a

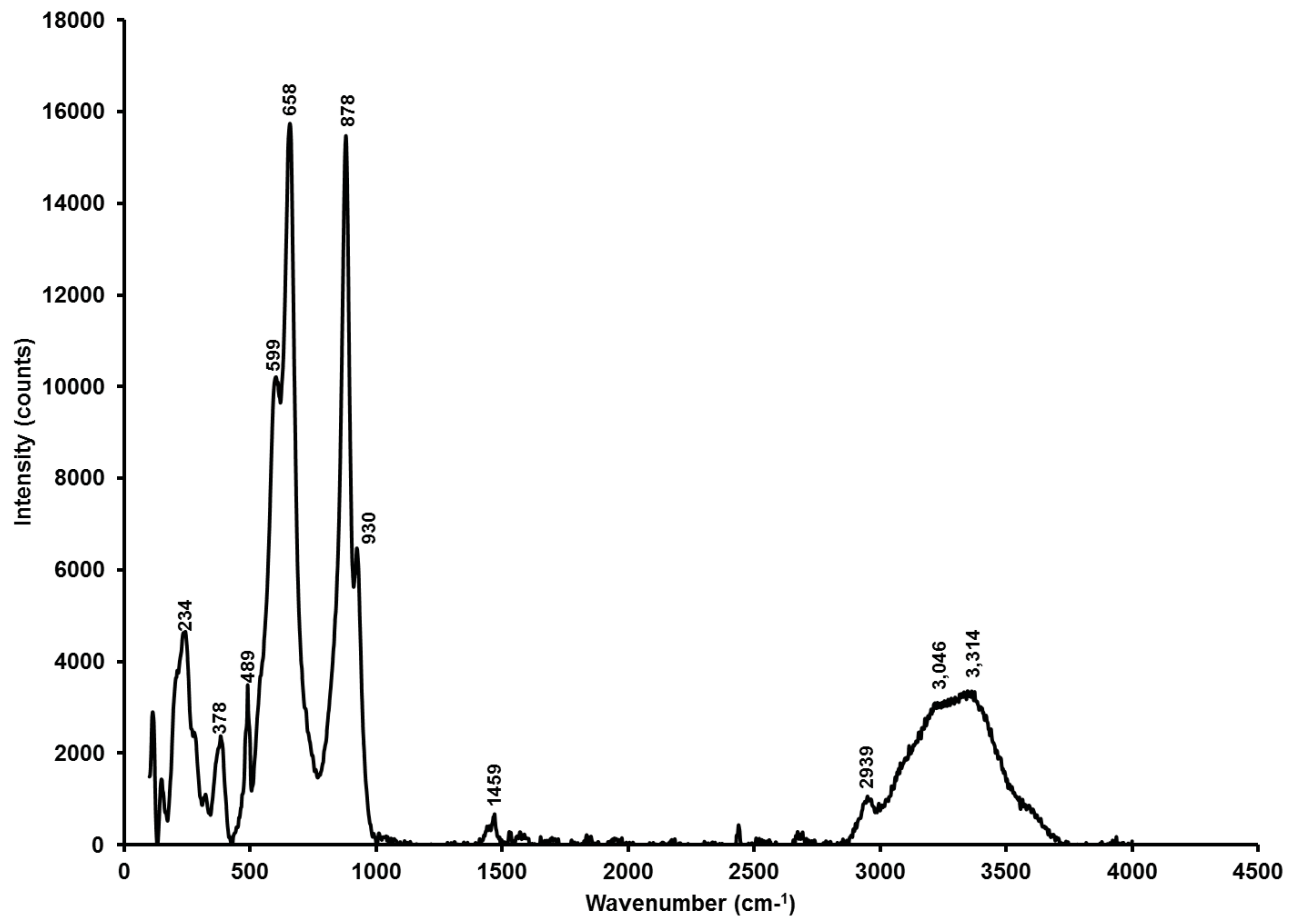


Figure 3b

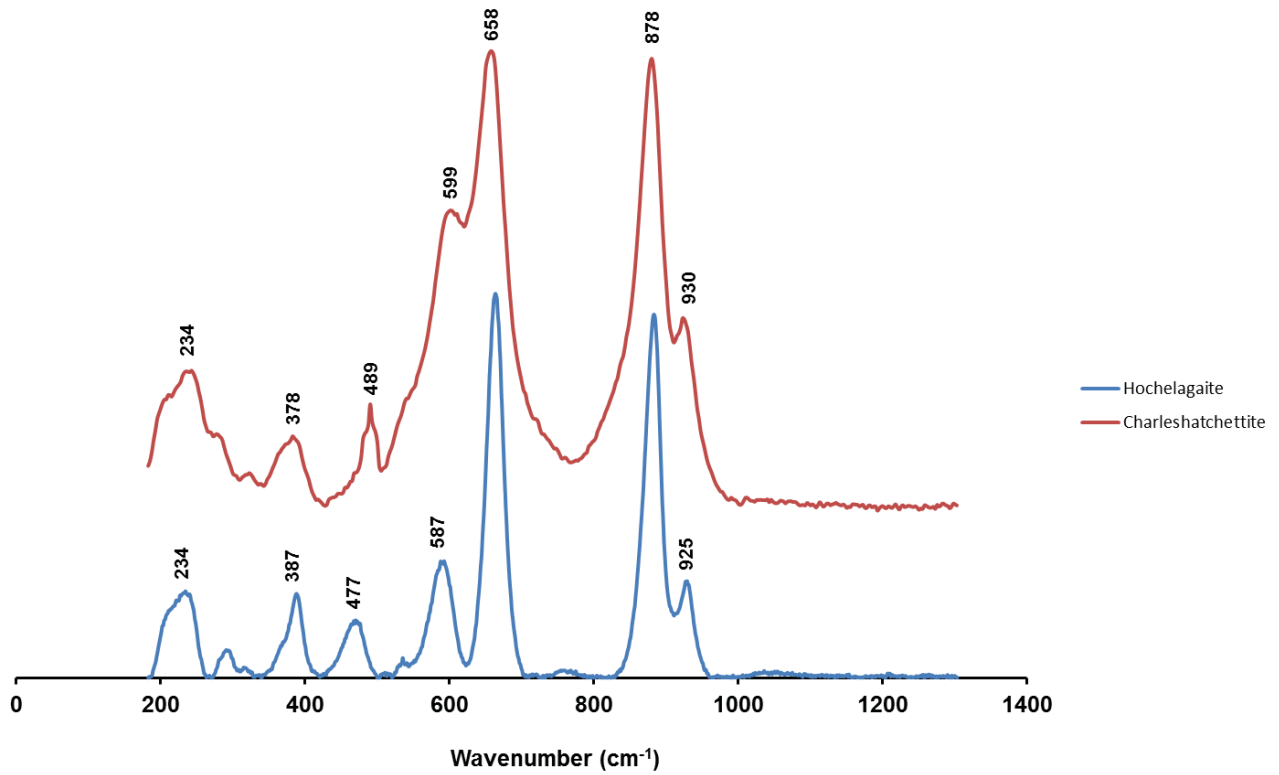


Figure 4

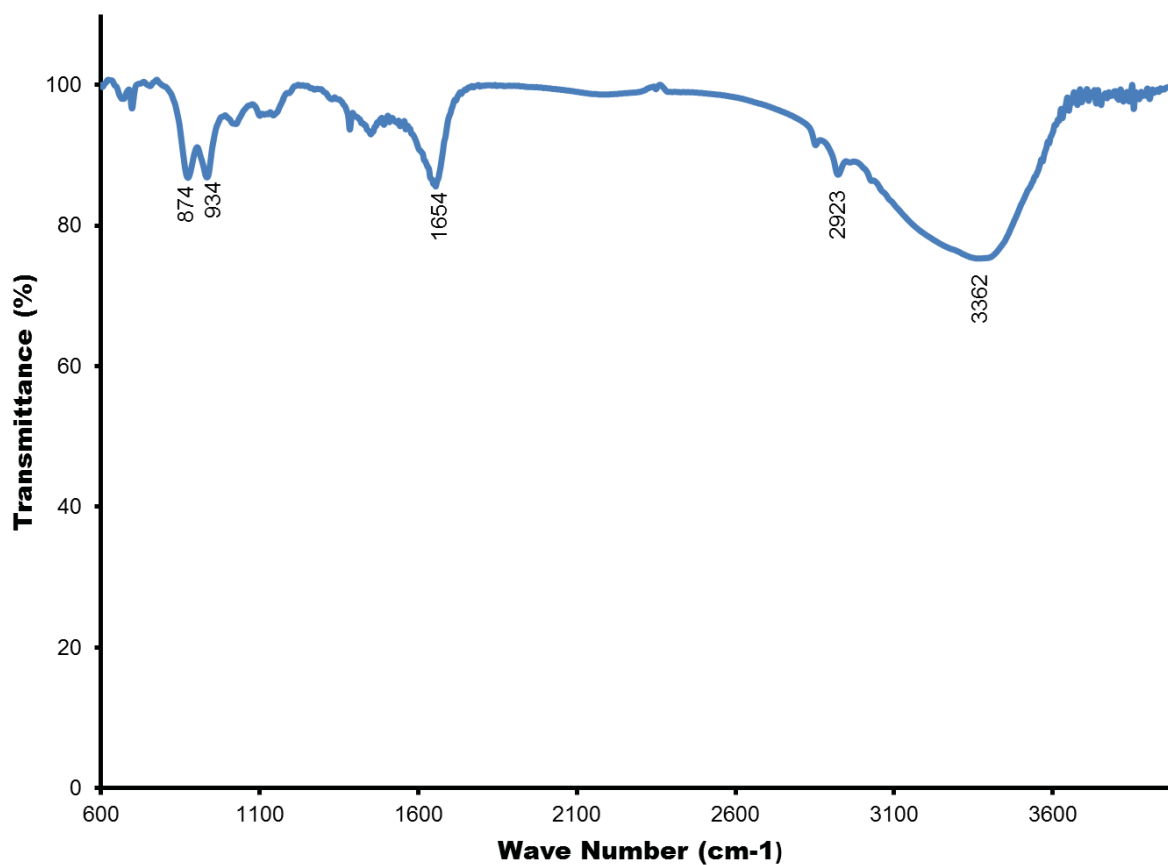


Figure 5

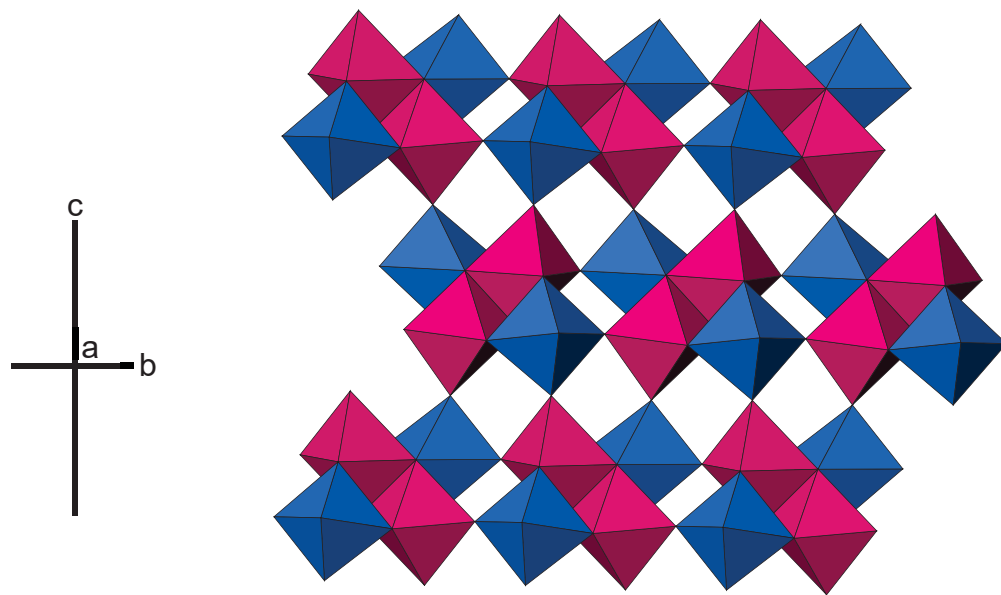


Figure 6

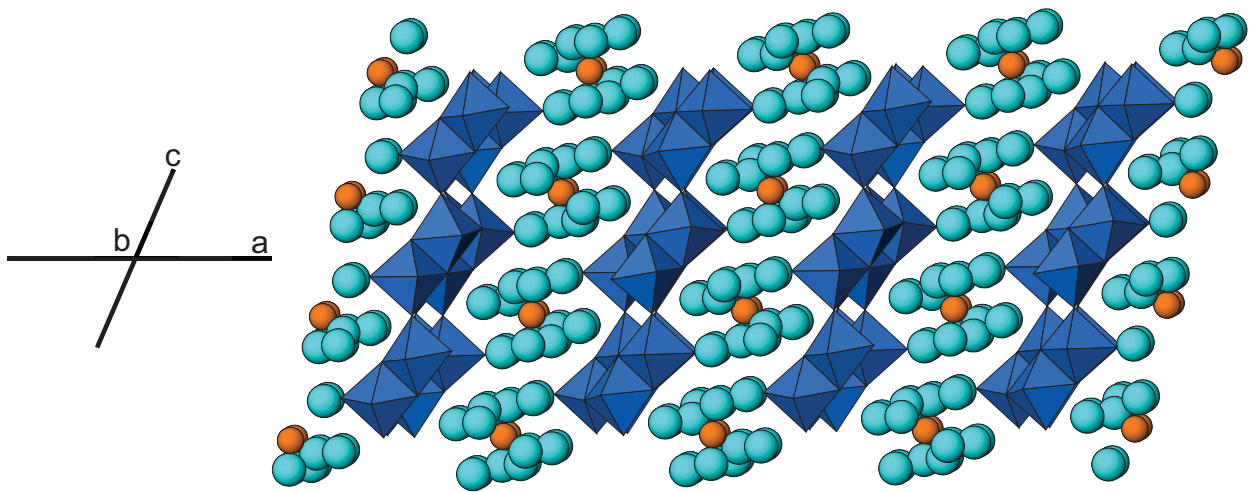


Table 1. Observed Raman absorption bands for charleshatchettite and hochelagaite.

<u>Hochelagaite*</u>	<u>Charleshatchettite</u>				
<u>Peak Position (cm⁻¹)</u>	<u>Peak Position (cm⁻¹)</u>	<u>Peak Position calc. (cm⁻¹)</u>	<u>Width</u>	<u>Intensity</u>	<u>Assignment</u>
	3314		Broad	Mod.Strong	O-H bending
	3046		Broad	Mod. Strong	O-H bending
	2939		Mod. Sharp	Weak	O-H bending
	1459		Mod. Sharp	Weak	H-O-H bending
925	930	946	Sharp	Mod. strong	Symmetric stretching of Nb=O double bond
878	878	855	Sharp	Very strong	Symmetric stretching of Nb=O double bond
663	658	678	Sharp	Very strong	Nb-O-Nb linkages – symmetric stretching
587	599	607	Sharp	Mod. strong	Nb-O-Nb linkages – symmetric stretching
477	489	455	Mod. Sharp	Weak	Ca-O
387	378	355	Mod. Sharp	Weak	Ca-O
325	234	288	Sharp	Weak	Ca-O
300	215	-	Sharp	Mod. strong	Ca-O
234	205	183	Sharp	Weak	Ca-O
196	150	-	Mod. Sharp	Weak	Ca-O
-	115	-	Sharp	Mod. strong	Ca-O

* Raman data for hochelagaite from this study.

Table 2. FTIR peaks and peak assignments for charleshatchettite

<u>FTIR Transmittance band (cm⁻¹)</u>	<u>Suggested Assignment</u>
3362	O-H Bending
2923	O-H Bending
2852	O-H Bending
1654	H-O-H Bending
1450	H-O-H Bending
1384	Atmospheric CO ₂
1100	asymmetric Si-O stretching
1025	Symmetric stretching of Nb=O double bond
934	Symmetric stretching of Nb=O double bond
874	Symmetric stretching of Nb=O double bond
755	Nb-O-Nb linkages - symmetric stretching
697	Nb-O-Nb linkages - symmetric stretching
666	Nb-O-Nb linkages - symmetric stretching

Table 3. X-ray powder diffraction data for charleshattchettite and hochelagaite.

Charleshattchettite							Hochelagaite ¹					Charleshattchettite							Hochelagaite ¹				
<i>I</i> _{obs}	<i>I</i> _{calc}	<i>d</i> _{obs} (Å)	<i>d</i> _{calc} (Å)	<i>h</i>	<i>k</i>	<i>l</i>	<i>I</i> _{obs}	<i>d</i> _{obs} (Å) ¹	<i>h</i>	<i>k</i>	<i>l</i>	<i>I</i> _{obs}	<i>I</i> _{calc}	<i>d</i> _{obs} (Å)	<i>d</i> _{calc} (Å)	<i>h</i>	<i>k</i>	<i>l</i>	<i>I</i> _{obs}	<i>d</i> _{obs} (Å) ¹	<i>h</i>	<i>k</i>	<i>l</i>
100	100	10.308	10.263	2	0	0	100	10.00	2	0	0	20	4	2.697	2.69	2	2	2	5	2.693	4	4	0
																					-5	3	1
12	3	6.199	6.193	1	1	0	20	6.18	-1	0	1		1		2.684	1	1	4					
							<5	5.61	-1	1	1		13		2.676	7	1	-2					
							50	5.39	2	2	0	6	5	2.593	2.582	5	1	-4	5	2.606	3	4	1
14	12	5.165	5.132	4	0	0	50	4.96	4	0	0								20	2.541	7	0	1
																					-4	2	2
38	24	4.832	4.801	2	0	2													<5	2.492	5	4	0
39	30	4.731	4.711	3	1	0															7	1	1
							<5	4.61	3	2	0	5	1	2.283	2.277	7	1	2	10	2.276	5	2	2
16	2	4.556	4.539	1	1	-2							3		2.27	2	2	-4					
	12		4.517	4	0	-2													20	2.232	-2	4	2
							10	4.48	3	0	1	7	1	2.207	2.196	4	2	-4	<5	2.197	-6	4	1
5	5	4.244	4.22	1	1	2	20	4.24	3	1	1		6		2.193	9	1	-2			2	4	2
3	3	4.106	4.086	3	1	-2						2	2	2.166	2.152	9	1	0					
							20	3.93	2	3	0	4	1	2.12	2.117	2	0	-6					
									4	2	0		1		2.112	1	3	1					
							5	3.61	3	3	0	27	4	2.071	2.064	3	3	0	20	2.085	9	2	0
6	4	3.56	3.547	4	0	2							6		2.061	3	3	-1					
	1		3.534	5	1	-1							6		2.056	0	0	-6					
12	9	3.492	3.476	3	1	2	10	3.5	1	3	1	3	1	2.017	2.011	3	1	-6	20	2.02	-8	0	2
	2		3.47	5	1	0							2		2.002	2	2	-5					
15	1	3.352	3.355	6	0	-2													30	1.979	-2	5	2
	13		3.329	5	1	-2						7	3	1.934	1.929	2	0	6					

25	10	3.262	3.248	0	2	0													20	1.89	-4	6	1	
25	2	3.193	3.176	5	1	1	70	3.208	0	4	0	4	2	1.846	1.84	11	1	-2						
	16		3.173	2	0	-4							1		1.837	7	1	-6						
9	4	3.155	3.141	0	2	-1	5	3.161	1	4	0		1		1.837	11	1	-1						
24	10	3.108	3.097	2	2	0	80	3.115	0	1	2								5	1.81				
	11		3.085	0	0	-4						7	4	1.785	1.779	3	1	6						
7	5	3.068	3.057	2	2	-1	20	3.059	1	1	2		1		1.776	3	3	-4						
							<5	2.936	-4	3	1								20	1.755				
4	2	2.888	2.874	0	2	-2													10	1.708				
							<5	2.854	4	3	1	5	1	1.702	1.694	7	3	-3	10	1.69				
13	1	2.806	2.803	3	1	-4	40	2.799	-2	2	2		1		1.692	7	3	1						
	12		2.791	5	1	2							3		1.691	9	1	-6						
8	1	2.755	2.755	4	2	-1																		
	2		2.745	4	2	0																		
	4		2.74	7	1	-1																		

Table 4. Miscellaneous single crystal data for charleshatchettite.

a (Å)	21.151(4)	Monochromator	Graphite
b	6.496(2)	Intensity-data collection	$\theta:2\theta$
c	12.714(3)	Criterion for observed reflections	$F_o > 4\sigma(F_o)$
β (°)	103.96(3)	GoOF	1.188
V (Å ³)	1695.3(6)	total No. of reflections	4160
Space group	$C2/c$ (#2)	No. Unique reflections	1106
Z	4	R (merge %)	7.85
D_{calc} (g/cm ³)	2.878	R %	5.39
Radiation	MoK α (50 kV, 40 mA)	wR^2 %	13.89

Table 5. Crystallographic parameters for members of the franconite group.

	Charleshatchettite	Hochelagaite ¹	Franconite ²	Ternovite ³
<i>a</i> (Å)	21.151(4)	19.88(1)	10.119(2)	20.656
<i>b</i> (Å)	6.496(2)	12.83(1)	6.436(1)	13.062
<i>c</i> (Å)	12.714(3)	6.44(1)	12.682(2)	6.388
β (°)	103.96(3)	93.20(3)	99.91(3)	90.917
<i>V</i> (Å ³)	1695.3(6)	1655.89(1)	813.6(1)	1709.83
<i>Z</i>	4	4	4	4
Space Group	<i>C2/c</i> (#15)	unknown	<i>P2₁/c</i>	<i>P2/m, P2, Pm</i>

- 1) Jambor *et al.* 1986
- 2) Haring & McDonald 2014
- 3) Subbotin *et al.* 1997

Table 6. Positional and displacement parameters for charleshatchettite.

ATOM	<i>x</i>	<i>y</i>	<i>z</i>	SOF	U_{11}	U_{22}	U_{33}	U_{23}	U_{13}	U_{12}	U_{eq}
Ca	0	0.0718(6)	3/4	1	0.037(3)	0.010(2)	0.027(3)	0	0.002(2)	0	0.025(1)
Nb(1)	0.32608(6)	0.0272(2)	0.9119(2)	1	0.032(9)	0.0063(8)	0.0136(8)	0.0003(5)	0.0080(6)	0	0.0218(6)
Nb(2)	0.25153(7)	-0.4368(2)	0.8934(2)	1	0.040(2)	0.0086(9)	0.0175(9)	0.0001(5)	0.0088(7)	-0.0002(6)	0.0252 (2)
O(1)	0.4076(5)	0.082(2)	0.9162(8)	1	0.040(7)	0.013(5)	0.025(6)	0.001 (4)	0.004(5)	0.005(5)	0.027(2)
O(2)	0.3304(4)	0.0002(2)	1.0651(7)	1	0.030(6)	0.004(5)	0.013(5)	0.004(4)	0.001(4)	-0.001(4)	0.017(2)
O(3)	0.2844(5)	0.054(2)	0.7526(7)	1	0.045(6)	0.008(5)	0.012(5)	0.002(4)	0.010(5)	0.004(4)	0.021(2)
O(4)	0.3302(4)	-0.275(2)	0.8927(7)	1	0.035(6)	0.003(5)	0.018(5)	0.001(4)	0.007(5)	-0.003(4)	0.019(2)
O(5)	0.2916(5)	0.313(2)	0.9176(7)	1	0.043(7)	0.002(5)	0.019(5)	0.001(4)	0.010(5)	-0.004(4)	0.021(2)
OH(6)	0.2252(5)	-0.111(2)	0.9236(7)	1	0.045(7)	0.015(5)	0.024(6)	-0.004(4)	0.022(5)	-0.005(4)	0.026(2)
OW(7)	0.0499(7)	-0.021(2)	0.598(2)	1	0.089(1)	0.035(7)	0.038(8)	-0.015(6)	-0.001(7)	0.015(7)	0.056(4)
OW(8)	0.0103(5)	0.373(2)	0.8725(8)	1	0.049(7)	0.19(6)	0.031(6)	-0.003(5)	0.017(5)	0.002(5)	0.032(3)
OW(9a)	-0.063(2)	-0.229(5)	0.685(3)	0.63(2)	0.07(2)	0.03(2)	0.08(3)	-0.05(2)	0	0.01(2)	0.06(1)
OW(9b)	-0.058(4)	-0.253(2)	0.640(6)	0.37(3)	0.06(3)	0.10(4)	0.11(5)	-0.11(4)	0.03(3)	-0.01(3)	0.09(2)
OW(10)	0.1212(5)	0.165(2)	0.803(8)	1	0.046(7)	0.026(6)	0.032(6)	-0.006(5)	0.014(5)	-0.013(5)	0.034(3)

Table 7. Bond-valence table (*v.u.*) for charleshatchettite

	Ca	Nb1	Nb2	Σ
O1		1.537 ^{↓→}		1.537
O2		0.930 ^{↓→}	0.841 ^{↓→}	1.771
O3		0.763 ^{↓→}	1.245 ^{↓→}	2.008
O4		0.817 ^{↓→}	0.853 ^{↓→}	1.670
O5		0.780 ^{↓→}	1.265 ^{↓→}	2.045
OH6		0.312 ^{↓→}	0.784 ^{↓→}	1.096
OW7	0.480 ^{↓→}			0.480
OW8	0.498 ^{↓→}			0.498
OW9a	0.328 ^{↓→}			0.328
OW9b	0.178 ^{↓→}			0.178
OW10	0.408 ^{↓→}			0.408
Σ	1.891	5.139	4.988	

Table 8. Interatomic distances (Å) in charleshatchettite

<i>Ca</i> (H ₂ O) ₈ Polyhedron			<i>Nb</i> (2)O ₄ (OH) ₂ Octahedron		
<i>Ca</i>	-OW9 <i>b</i> x2	2.66(7)	<i>Nb</i> 2	-O3	1.828(9)
	-OW9 <i>a</i> x2	2.40(4)		-O5	1.823(9)
	-OW7 x2	2.49(2)		-O4	1.969(9)
	-OW8 x2	2.48(2)		-O2	1.972(9)
	-OW10 x2	<u>2.56(2)</u>		-OH6	2.248(9)
< <i>Ca</i>	-O>	2.518		-OH6	<u>2.281(9)</u>
			< <i>Nb</i> 2	-O>	2.020
<i>Nb</i> (1)O ₅ (OH) Octahedron					
<i>Nb</i> 1	-O1	1.749(2)			
	-O2	1.936(9)			
	-O5	2.004(8)			
	-O4	1.985(8)			
	-O3	2.012(9)			
	-OH6	<u>2.352(9)</u>			
< <i>Nb</i> 1	-O>	2.006			